TABLE 1. Strains used in this study

Strain	Genotype*
YVL3584	*MATa/α tlc1-Δ::HIS3/TLC1*
YVL3015	*MATa/α tlc1-Δ::HIS3/TLC1 tel1-Δ::kanMX6/TEL1*
YVL3597	*MATa/α tlc1-Δ::HIS3/TLC1 xrs2-Δ::kanMX6/XRS2*
YVL3782	*MATa/α tlc1-Δ::HIS3/TLC1 xrs2-Δ::natMX4/XRS2 tel1-Δ::kanMX6/TEL1*
YVL3706	*MATa/α tlc1-Δ::HIS3/TLC1 rad50-Δ::natMX4/RAD50*
YVL3873	*MATa/α tlc1-Δ::HIS3/TLC1 rad50-Δ::natMX4/RAD50 tel1-Δ::kanMX6/TEL1*
YVL3568	*MATa/α tlc1-Δ::HIS3/TLC1 rif2-Δ::kanMX6/RIF2*
YVL3707	*MATa/α tlc1-Δ::HIS3/TLC1 rif2-Δ::kanMX6/RIF2 rad50-Δ::natMX4/RAD50*
YVL3698	*MATa/α tlc1-Δ::HIS3/TLC1 rif2-Δ::kanMX6/RIF2 xrs2-Δ::natMX4/XRS2*
YVL3697	*MATa/α tlc1-Δ::HIS3/TLC1 rif2-Δ::natMX4/RIF2 tel1-Δ::kanMX6/TEL1*
YVL3852	*MATa/α tlc1-Δ::HIS3/TLC1 rad51-Δ::natMX4/RAD51 rad50-Δ::kanMX6/RAD50*
YVL3708	*MATa/α tlc1-Δ::HIS3/TLC1 rad51-Δ::natMX4/RAD51 rif2-Δ::kanMX6/RIF2*
YVL3705	*MATa/α tlc1-Δ::HIS3/TLC1 rad51-Δ::natMX4/RAD51 tel1-Δ::kanMX6/TEL1*
YVL3851	*MATa/α tlc1-Δ::HIS3/TLC1 rad52-Δ::natMX4/RAD52 rad50-Δ::kanMX6/RAD50*
YVL3288	*MATa/α tlc1-Δ::HIS3/TLC1 rif1-Δ::natMX4/RIF1*
YVL3619	*MATa/α tlc1-Δ::HIS3/TLC1 rif1-Δ::natMX4/RIF1 rif2-Δ::kanMX6/RIF2*
YVL3785	*MATa/α tlc1-Δ::HIS3/TLC1 rif1-Δ::natMX4/RIF1 tel1-Δ::kanMX6/TEL1*
YVL3608	*MATa/α tlc1-Δ::HIS3/TLC1 sae2-Δ::kanMX6/SAE2*
YVL3620	*MATa/α tlc1-Δ::HIS3/TLC1 sae2-Δ::kanMX6/SAE2 sgs1-Δ::kanMX6/SGS1*
YVL3696	*MATa/α tlc1-Δ::HIS3/TLC1 sae2-Δ::kanMX6/SAE2 tel1-Δ::natMX4/TEL1*

additional genotype: *ura3*-52/*ura3*-52 *lys2*-801/*lys2*-801 *trp1*-Δ1/*trp1*-Δ1 *his3*-Δ200/*his3*-Δ200 *leu2*-Δ1/*leu2*-Δ1

All strains used in this study, as well as prior publications from our lab on replicative senescence, are isogenic to YVL3584, which is derived from YNN216 (with *ade2-101* converted to *ADE2* by gene replacement); see http://wiki.yeastgenome.org/index.php/Commonly_used_strains#S288C for more information.

(A)

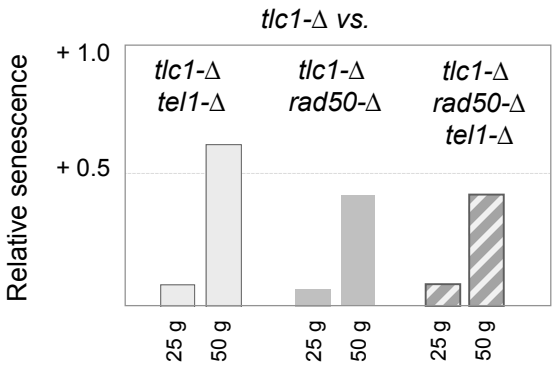

(B)

	Expt.	~25 g	~50 g
tlc1-Δ *tel1*-Δ *vs.* *tlc1*-Δ *tel1*-Δ *xrs2*-Δ	I	0.9	0.3
	II	0.2	0.2
tlc1-Δ *tel1*-Δ *vs.* *tlc1*-Δ *tel1*-Δ *rad50*-Δ	I	0.6	0.2
	II	0.6	0.2

Fig. S1. Tel1 and the MRX complex act in the same pathway to modulate senescence. (A) Relative senescence scores for the indicated double and triple mutant strains (correponding to 23, 28 and 26 isolates for each of the three genotypes, respectively), normalized to the senescence score for a *tlc1*-Δ strain (29 isolates); all isolates were generated from a single diploid strain following dissection. A second independent experiment (comparing 18, 34 and 37 double and triple mutant isolates to 29 *tlc1*-Δ isolates) yielded essentially identical results (data not shown). (B) Summary of the *p*-values when comparing senescence scores for the triple mutant strains (*tlc1*-Δ *tel1*-Δ *xrs2*-Δ or *tlc1*-Δ *tel1*-Δ *rad50*-Δ) with that of the isogenic *tlc1*-Δ *tel1*-Δ strain, which demonstrates no significant difference between the growth phenotypes of the triple and double mutants, for each of two independent experiments.

(A)

		25 g	50 g	75 g
	Expt.			
tlc1-Δ *rad50*-Δ *vs.*	I	0.9	0.8	0.3
tlc1-Δ *rad50*-Δ *rif2*-Δ	II	0.9	0.2	0.3

(B)

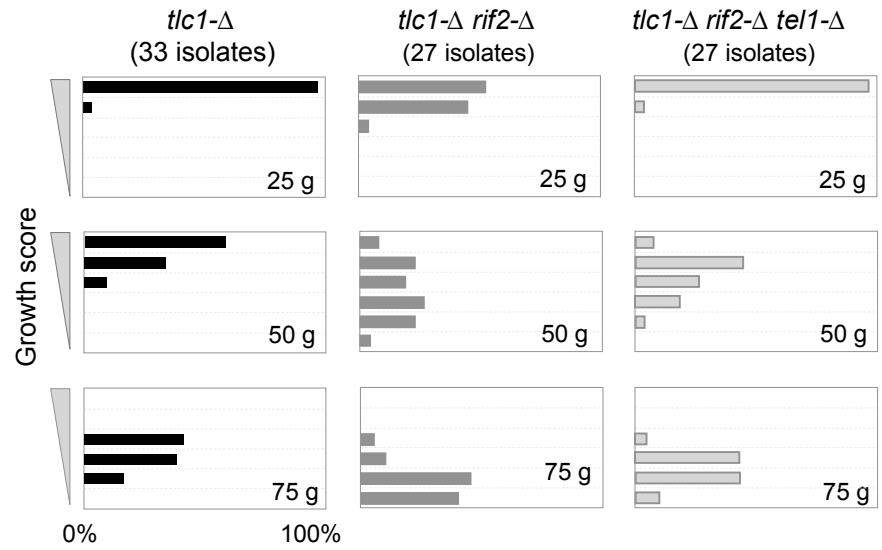

Fig. S2. Rif2 acts upstream of the MRX complex to regulate replicative senescence. (A) Summary of *p*-values when comparing the senescence scores for *tlc1*-Δ *rad50*-Δ and *tlc1*-Δ *rad50*-Δ *rif2*-Δ strains for two independent experiments. (B) An independent repeat of the *rif2*-Δ *tel1*-Δ epistasis shown in Fig. 3C, which demonstrates that loss of Tel1 partially reverses the accelerated senescence observed in *tlc1*-Δ *rif2*-Δ strains.

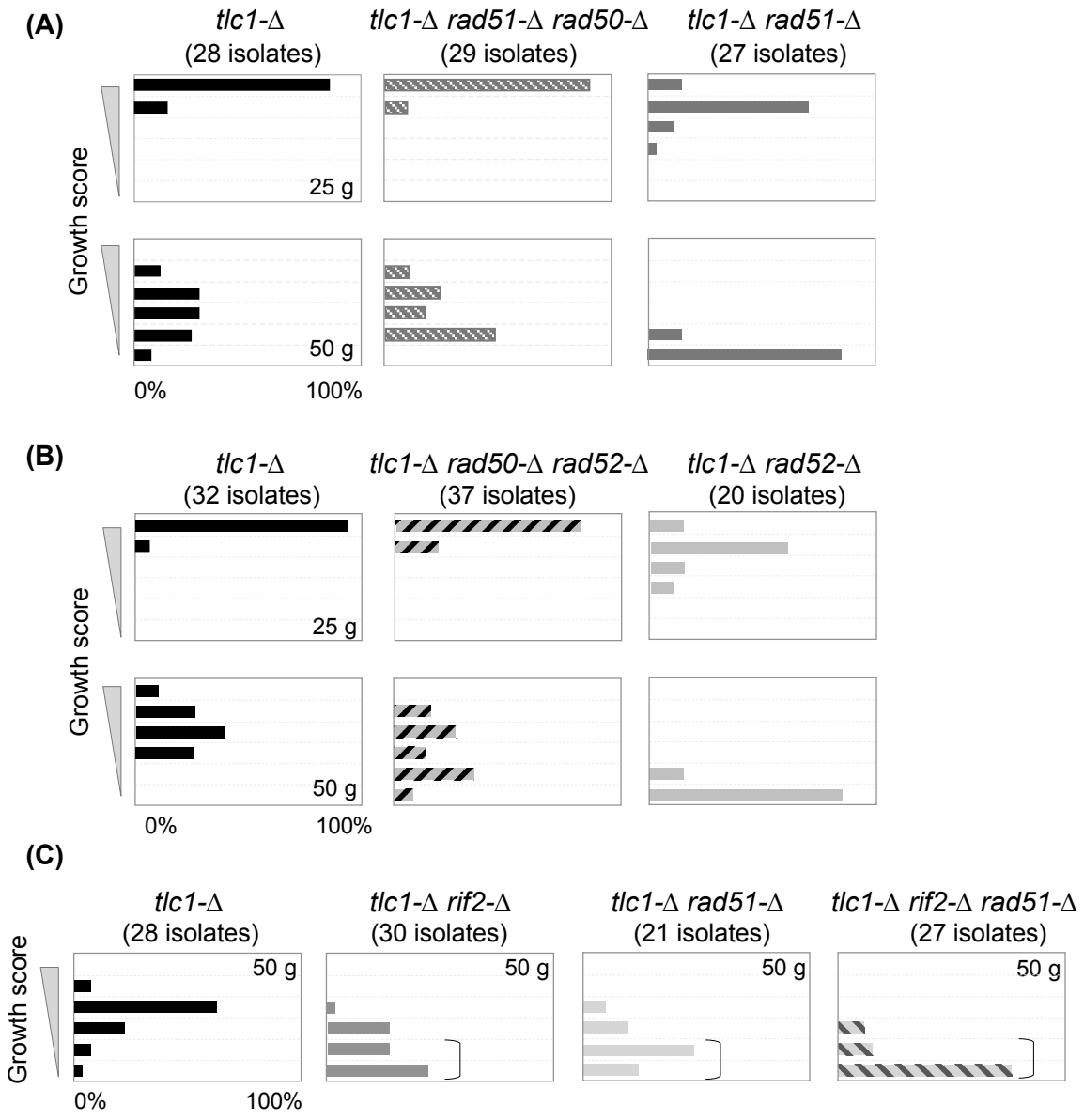

Fig. S3. Rad50 and Rad52 contribute to senescence through pathway(s) that are distince from the MRX pathway. (A) and (B) Senescence profiles corresponding to the experiments shown in Fig. 4A and B. (C) Senescence profiles at 50 generations for telomerase-defective strains derived from a *tlc1-Δ/TLC1 rif2-Δ/RIF2 rad51-Δ/RAD51* diploid, which demonstrates that senescence is so accelerated that the majority of the double and triple mutant isolates scored in the bottom two categories (indicated by brackets), corresponding to a nearly complete loss of viabiity.

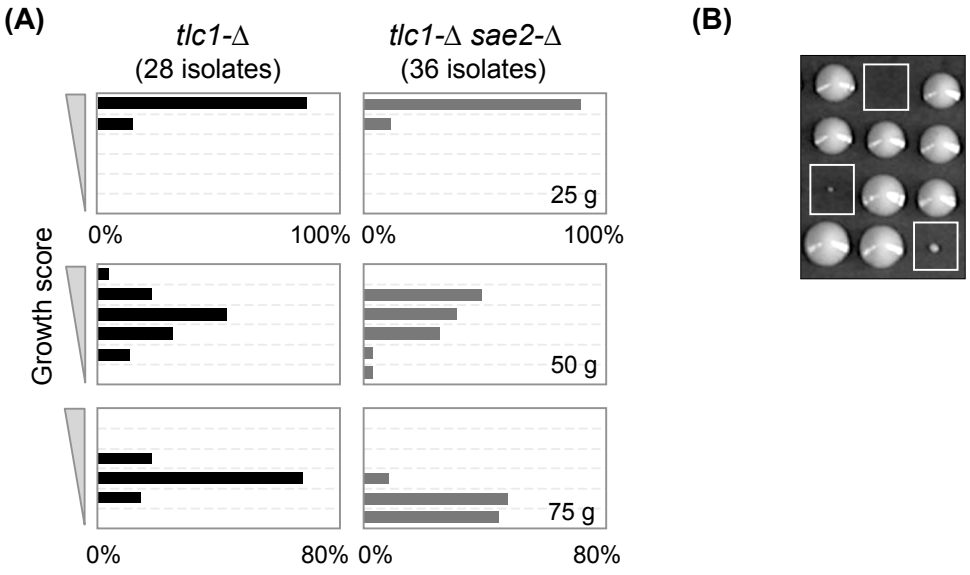

Fig. S4. Phenotypic consequences of a *sae2*-Δ null mutation in strains that lack telomerase or Sgs1. (A). Histogram of the senescence profile of 28 isolates of *tlc1*-Δ vs. 36 isolates of *tlc1*-Δ *sae2*-Δ, which illustrates that loss of *SAE2* function only becomes evident late in the growth of a telomerase-defective strain. (B) Viability of spores from three tetratype tetrads following sporulation of a *sae2*-Δ*/SAE2 sgs1*-Δ*/SGS1* diploid, following growth for three days at 30°; the *sgs1*-Δ *sae2*-Δ spore colonies are indicated by white boxes.

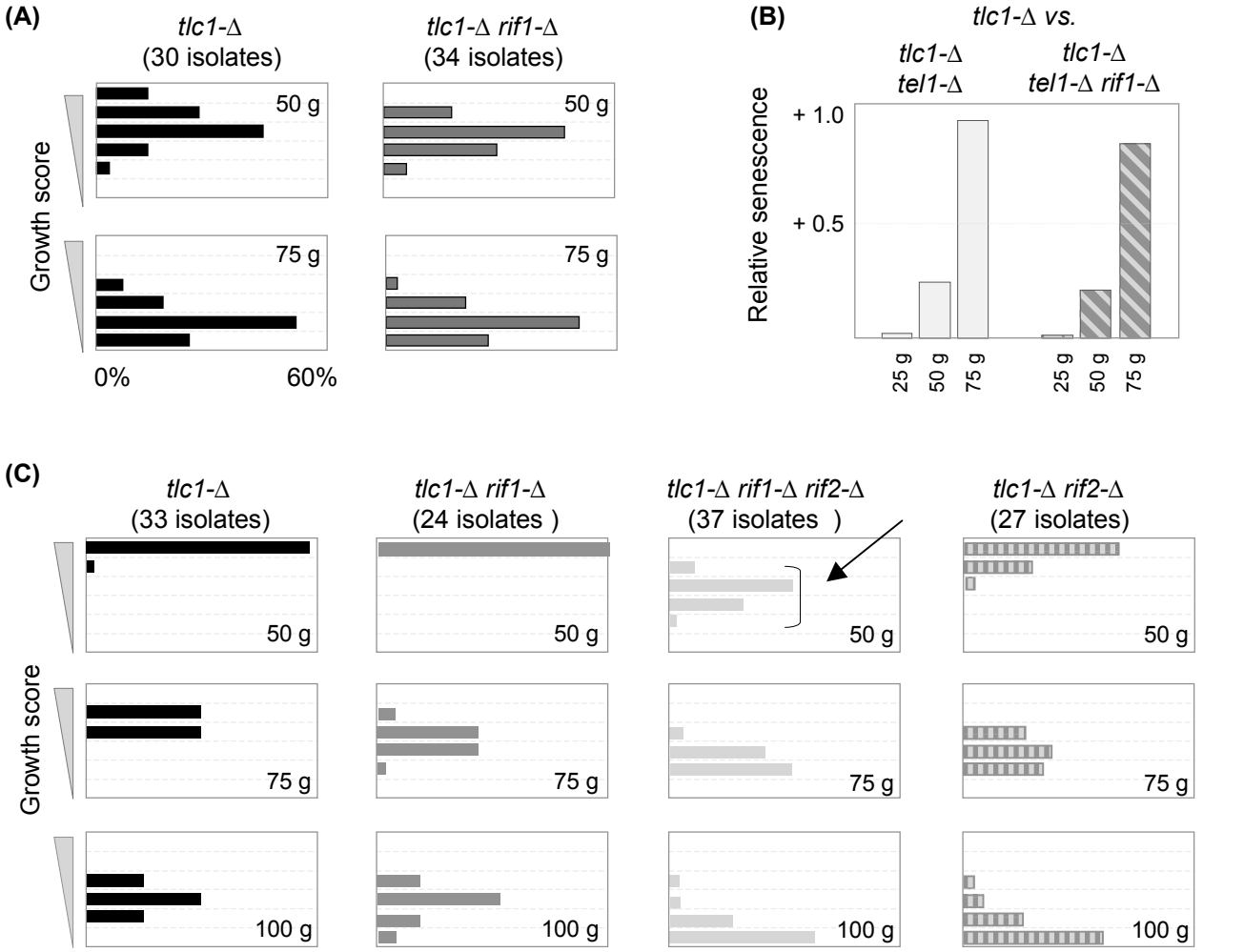

(D)

		25 g	50 g
	Expt.		
tlc1-Δ *rif2*-Δ *vs.* *tlc1*-Δ *rif2*-Δ *rif1*-Δ	I	< 0.001	0.3
	II	0.005	0.2

(E)

		50 g	75 g	100g
	Expt.			
tlc1-Δ *vs.* *tlc1*-Δ *rif1*-Δ	I	0.4	0.9	0.5
	II	0.8	0.2	0.7

Fig. S5. Rif1 contributes to replicative senescence transiently, and only in the absence of Rif2. (A) A comparison of the senescence profiles of *tlc1*-Δ and *tlc1*-Δ *rif1*-Δ shows that loss of Rif1 function has no impact on the progressive growth decline of a *tlc1*-Δ strain. (B). Similarly, a *rif1*-Δ mutation does not alter the senescence behavior of a *tlc1*-Δ *tel1*-Δ strain. (C) Loss of both Rif1 and Rif2 imposes a transient growth defect early in the outgrowth of a telomerase-defective strain (indicated by the bracket and arrow). (D) *p*-values comparing *tlc1*-Δ *rif2*-Δ with *tlc1*-Δ *rif2*-Δ *rif1*-Δ demonstrates that the additive effect at the 25 generation time point is statistically significant in two independent experiments. (E) *p*-values comparing *tlc1*-Δ with *tlc1*-Δ *rif1*-Δ, for two independent experiments (one of which is shown in part C), where the haploid isolates were from a *tlc1*-Δ/*TLC1 rif1*-Δ/*RIF1 rif2*-Δ/*RIF2* strain.